Structure, Vol. 12, 477–486, March, 2004, ©2004 Elsevier Science Ltd. All rights reserved. DOI 10.1016/j.str.2004.02.006

ADP-Ribosyl Cyclase: Crystal Structures Reveal a Covalent Intermediate

Michael L. Love,[1] Doletha M.E. Szebenyi,[1] Irina A. Kriksunov,[1] Daniel J. Thiel,[1] Cyrus Munshi,[2] Richard Graeff,[2] Hon Cheung Lee,[2,*] and Quan Hao[1,*]

[1]Molecular Biology and Genetics
Cornell University
Ithaca, New York 14853

[2]Department of Pharmacology
University of Minnesota
Minneapolis, Minnesota 55455

Summary

ADP-ribosyl cyclase catalyzes the elimination of nicotinamide from NAD and cyclization to cADPR, a known second messenger in cellular calcium signaling pathways. We have determined to 2.0 Å resolution the structure of *Aplysia* cyclase with ribose-5-phosphate bound covalently at C3′ and with the base exchange substrate (BES), pyridylcarbinol, bound to the active site. In addition, further refinement at 2.4 Å resolution of the structure of nicotinamide-bound cyclase, which was previously reported, reveals that ribose-5-phosphate is also covalently bound in this structure, and a second nicotinamide site was identified. The structures of native and mutant Glu179Ala cyclase were also solved to 1.7 and 2.0 Å respectively. It is proposed that the second nicotinamide site serves to promote cyclization by clearing the active site of the nicotinamide byproduct. Moreover, a ribosylation mechanism can be proposed in which the cyclization reaction proceeds through a covalently bound intermediate.

Introduction

ADP-ribosyl cyclase catalyzes the elimination of nicotinamide from NAD and the production of second messenger cADPR (Lee et al., 1994 and reviewed in Lee, 2001). cGMP-activated kinase can stimulate the cyclase activity (Willmott et al., 1996), which is essential to the process of calcium-induced calcium release (CICR), a key component of the calcium signaling mechanism which controls cellular development. The propagation of this calcium signal component has been studied in sea urchin egg preparations (Lee 1991, 1996; Lee et al., 1995), and cyclase has been implicated in CICR potentiation (Lee et al., 1993, 1995). The enzyme is a 29 kDa protein and crystallizes as a functionally relevant dimer (Prasad et al., 1996), and is similar to BST-1, a cell surface antigen which has been implicated in severe rheumatoid arthritis (Kaisho et al., 1994; Dong et al., 1994; Itoh et al., 1994; Yamamoto-Katayama et al., 2002). The cyclase dimer is a model for surface antigen CD38, which may play a role in various immune system functions (States et al., 1992; Jackson and Bell, 1990; Harada et al., 1993; Koguma et al., 1994; Li et al., 1994). CD38 and ADP-ribosyl cyclase catalyze similar reactions, and the amino acid sequences are 30% identical. In the dimer, the substrate binding grooves are turned inward toward a central channel or cavity so that they are somewhat hidden from the solvent. It has been suggested that a channel, which is formed in the dimer, provides access to the catalytic core for substrates. The channel is large enough for products and reagents, as well as water and various ions, so it is unlikely that hydrolysis of intermediates is blocked by the constraints of the channel space topology. Moreover, channel access would of course be required for mechanism-based inhibitors which have been shown to block cyclization in CD38 (Sauve and Schramm, 2002).

Here we report the crystallographic structures of ADP-ribosyl cyclase covalently bound to C3′ of ribose-5-phosphate (R5P), in complex with pyridylcarbinol and nicotinamide respectively. In addition, the native cyclase structure was determined to 1.7 Å resolution, which is the highest resolution to date for the cyclase family, and the structure of the Glu179Ala cyclase mutant was also solved. The kinetic competence of cyclase to hydrolyze nicotinamide mononucleotide to R5P and nicotinamide was demonstrated by HPLC analysis. Based on a structural overlay of conserved residues, it appears that the overall topology of the dimer protects the substrate binding surfaces from proteolysis and blocks nonspecific access to the active site. In contrast to structures which were previously reported (Prasad et al., 1996; Yamamoto-Katayama et al., 2002), the R5P ribose ring is covalently linked to Glu179, the so-called catalytic residue of the BES-bound structures, so that the interaction of ribose-5-phosphate with a site adjacent to the pyridylcarbinol and nicotinamide site is revealed, and an enzymatic mechanism can be proposed which includes a covalent intermediate.

Results and Discussion

Overview of the Structure

The structures of ADP-ribosyl cyclase with bound pyridylcarbinol or nicotinamide BES (Munshi et al., 1999) are highly similar to those of mutant and native cyclase, except that no reagents were bound to the active site in either the mutant or native case. Although the 1.7 Å resolution structure was obtained from crystals grown in the presence of NGD, no bound substrate was found, and this structure is considered as native cyclase. In the case of the BES-bound structures, cyclization substrate reagents were not added to the crystallization mixture, so that the bound substrate or R5P was apparently co-purified with the protein; in the absence of nicotinamide or pyridylcarbinol, the R5P was apparently hydrolyzed away. A similar effect has been observed with the NAD^+-dependent deacetylase enzyme, SIR2: BES favors the accumulation of a covalent intermediate (Sauve and Schramm, 2003). The current structures are all similar to the first crystallographic structure of cyclase (Prasad

*Correspondence: qh22@cornell.edu (Q.H.), leehc@tc.umn.edu (H.C.L.)

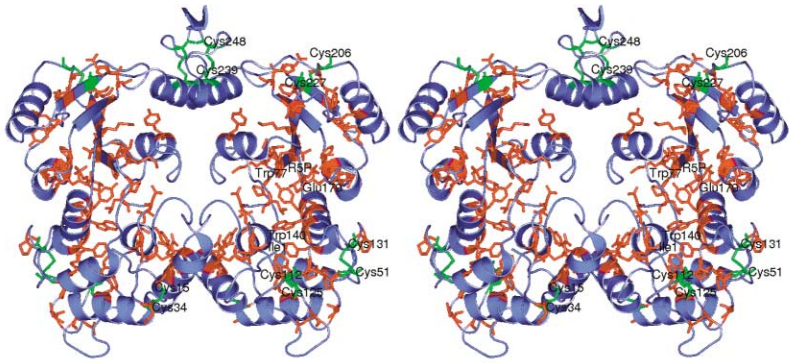

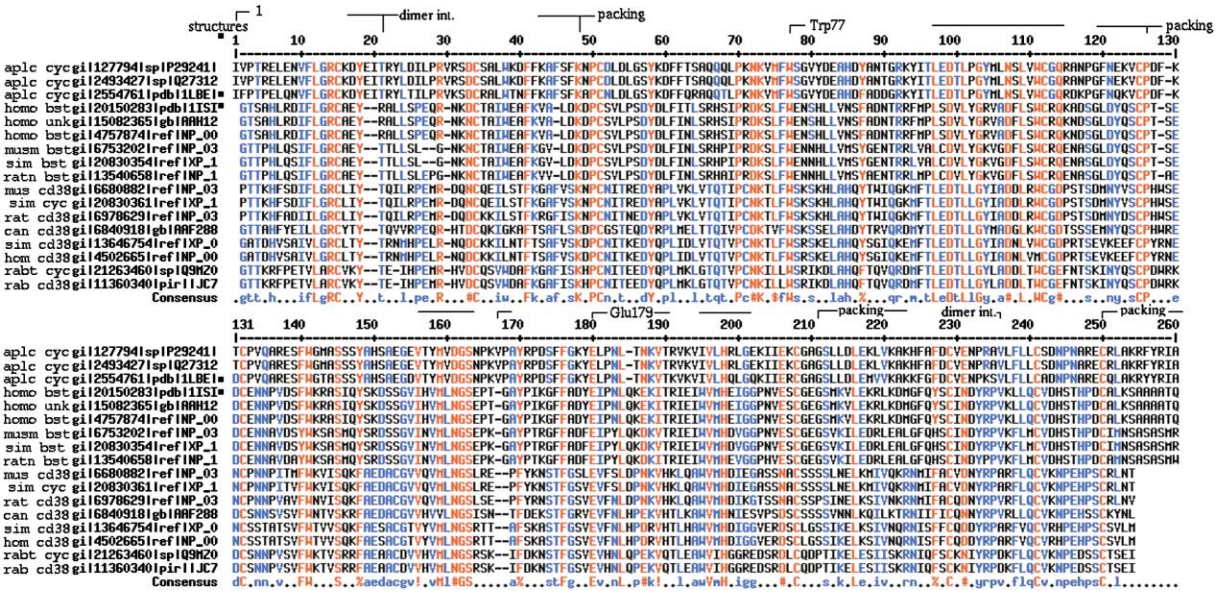

Figure 1. Conserved Structure

The cyclase dimer is shown in a stereo diagram. Residues shown in red are highly conserved in a sequence alignment of ADP ribosyl cyclase, BST-1, and CD38. Disulfide bonds are shown in green, and they are also conserved. Sequences of various cyclase (cyc), BST-1 (bst), and CD38 (cd38) molecules are shown in a truncated aligned stack with highly conserved residues shown in red. It is clear that many conserved residues are clustered near the catalytic cleft of each monomer. The figure was rendered with the program PyMOL (http://pymol.sourceforge.net).

et al., 1996; Munshi et al., 1999) and to each other with Cα rms differences of about 1 Å or less, and somewhat similar to the recently solved structure of BST-1 (Yamamoto-Katayama et al., 2002) with a Cα rms difference of about 3.5 Å. With respect to these earlier structures, improvements in crystallographic resolution together with crucial differences of bound substrates are found in the current structures.

A careful delineation of the dimeric topology and subdomain structure of the cyclase monomer assists with the mechanistic interpretation of its enzyme activity. A structural overlay of sequence similarity data within the cyclase family (comprising cyclase, CD38, and BST-1) shows that conserved residues are clustered in the dimeric cavity, especially in the substrate binding clefts (Figure 1). This region of the protein corresponds to a region that we have called the "substrate handler," and it encompasses most of the individual residues which have been found to affect enzymatic activity. This handler is intermediate between two large subdomains at the N- and C termini of the protein (Figure 2), an α unit and an αβ unit. The handler provides most of the binding surface for the bulky side chains of the substrate and so determines the relative specificity of the enzyme. Key residues of the handler are nestled deep in the dimeric cavity and cleft, and such an arrangement would impede proteolysis affecting enzymatic activity, and block nonspecific access to the hydrolyzing power of the active site.

Although the α and αβ units are less conserved than the handler, those residues which are conserved are clustered in regions of dimer interaction or scaffolding for the handler unit. In addition, the loops of both the α and αβ units contain conserved disulfide bonds, which hold the domains securely, and are likely to impede proteolysis of the exterior loops. Loops 1 and 2 of the α unit both have conserved regions, which provide crucial underpinning for the handler unit, while helices B and C are more divergent. With a deeply buried β strand, the αβ unit provides extensive scaffolding, so that residues

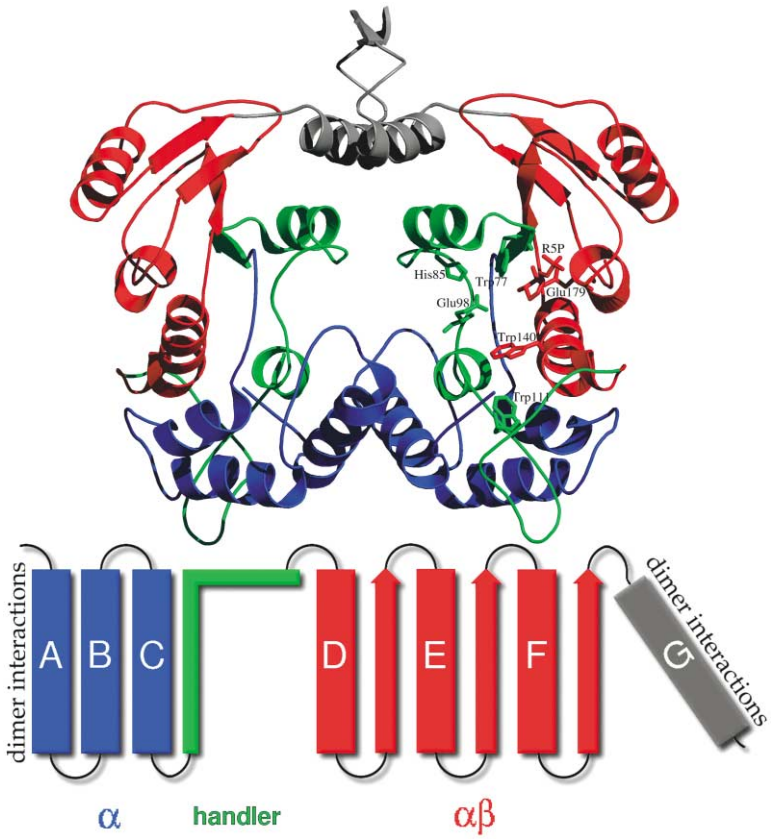

Figure 2. Subdomain View of Cyclase with Schematic Representation

The cyclase dimer is shown in a ribbon diagram with key structural components colored blue to green to red to gray from the N to the C terminus. Within one of the two cyclase molecules in the symmetrical dimer, residues which appear to play a role in the enzymatic activity are shown in stick representation. A convenient schematic view shows the coloring scheme that we have used for cyclase subdomain structure in the current study.

Glu179 and Trp140 can be positioned precisely for catalysis (Figure 3). A C-terminal helix bridges the dimer tail with conserved interactions.

Strikingly, R5P is largely buried in the core of the substrate binding groove and interacts with residues which are thought to be critical to the catalytic function

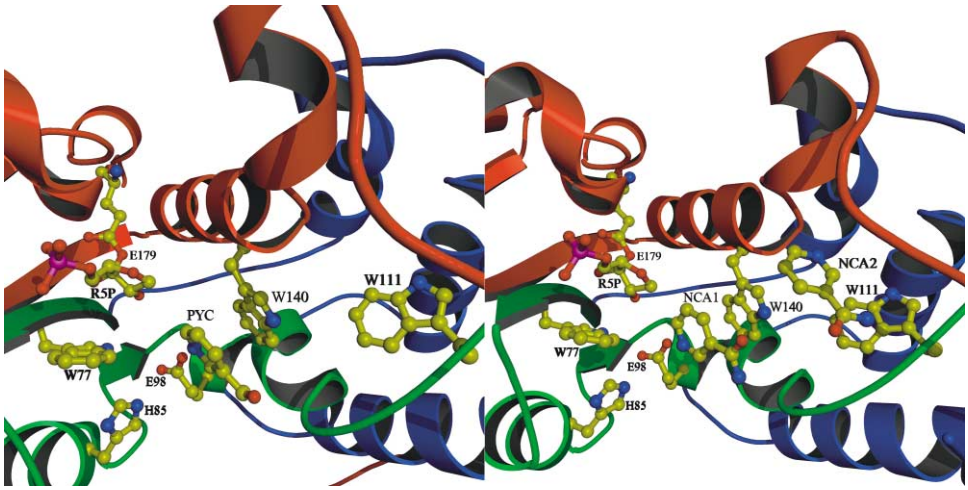

Figure 3. Cyclase Active Site with Bound Substrates, R5P, Pyridylcarbinol, and Nicotinamide

The three domains of ADP ribosyl cylcase are shown in ribbon representation and colored from N to C, blue, green, and red respectively. Key residues of the active site are shown in ball-and-stick representation, with the atoms colored as follows: C, yellow; N, blue; O, red; and P, violet. In the structure, R5P is covalently linked at the C3′ atom of the ribose ring to a carboxylate O of E179. The BES, pyridylcarbinol (PYC, left) or nicotinamide (NCA1, right), makes contact with E98 and is bound to W140 in the catalytic cleft. At right, W111 forms a second nicotine amide site (NCA2), which may shunt nicotine amide away from the active site in the course of the ADPr cyclization reaction. Together with the absence of bound R5P in the active site of the native structure, the results of this study show how BES compounds block cyclization and hydrolysis of the covalent intermediate. The figure was rendered with the program Povscript (http://dipsy.biochem.med.umich.edu/~peisach/povscript/) (see Kraulis, 1991).

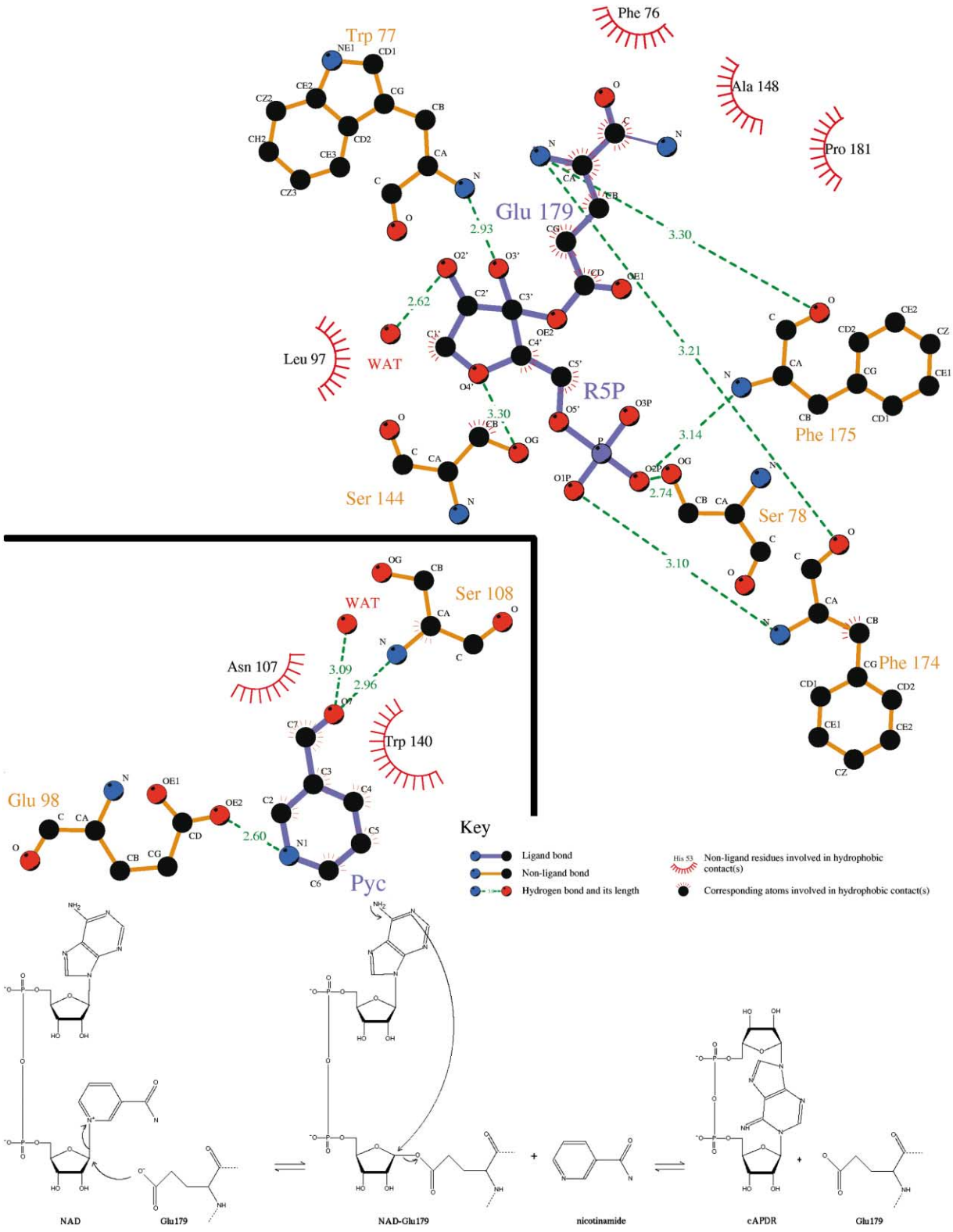

Figure 4. Schematic Representation of Cyclase Ligands and Reaction Mechanism

The interaction of cyclase residues with R5P-Glu179 and pyridylcarbinol (Pyc) are shown in a schematic representation (top). The figure was made with Ligplot (Wallace et al., 1995). The proposed reaction mechanism is also shown. The covalent intermediate in the current structure apparently accumulates when there is an excess of nicotinamide or pyridylcarbinol, which blocks the cyclization step.

of the enzyme. The sugar group interacts with the main chain amine of Trp77 and the phosphate interacts with the sidechain of S78, so that R5P is held away from the hydrophobic sidechain of Trp77. Moreover, the covalently linked Glu-R5P residue spans a helix comprising residues 173–180, which interacts with the sugar residue along its length, and the phosphate group forms two hydrogen bonds with the N terminus of the helix (Figure 4). Although it is likely that the formation of the C3′ covalent bond to Glu179 results in the elimination of the 3′ hydroxyl, it is visible in the map and included in the structure. The appearance of this hydroxyl group in the electron density is probably due to the presence of a C1′ or C2′ bound covalent intermediate at lower occupancy (see Structural Analysis section below), which could not be distinguished from the C3′ bound intermediate observed in the current structure at the resolution of the data. Thus, it appears that the handler and $\alpha\beta$ unit structures of cyclase provide for precise geometric orientation of the substrate and catalytic residues.

Hydrolysis of Nicotinamide Mononucleotide

The finding of R5P covalently bound to Glu179 is unexpected, and the substrate was apparently copurified with the enzyme. Although this observation of R5P might be explained as disorder in the second phosphate and purine group of a bound NAD, it is also possible that R5P is derived from the hydrolysis of nicotinamide mononucleotide (NMN), which cannot undergo the cyclization reaction. The competence of cyclase to catalyze the hydrolysis of NMN was tested by HPLC analyses as shown in Figure 5. After incubation of NMN with the cyclase, a portion was indeed hydrolyzed to nicotinamide (Figure 5A). This was further confirmed by measuring the time course of release of R5P from NMN during the hydrolysis reaction as shown in Figure 5B. Cyclase is a multifunctional enzyme capable of using different substrates, NAD and NADP, to produce structurally distinct products, cADPR and NAADP, respectively (Aarhus, et al. 1995). It is thus not surprising that it can also catalyze the hydrolysis of NMN to R5P. Indeed, a similar hydrolysis reaction has been shown to be catalyzed by CD38 (Sauve and Schramm, 2002; Sauve et al., 2000), the mammalian homolog of the cyclase. The covalently bound R5P observed in the cyclase crystals thus represents the first and definitive evidence that this hydrolysis reaction occurs via a covalent intermediate.

Structural Analysis

A key feature of the pyridylcarbinol- and nicotinamide-bound structures is the presence of R5P covalently bound to Glu179, the "catalytic residue" (Sauve et al., 2000). It may appear as puzzling that the covalent bond to Glu179 occurs at the C3′ position of R5P, as the proposed reaction mechanism involves C1′ (Figure 4). We propose that the existence of the C3′-Glu179 bond implies that covalent bond chemistry can also proceed with Glu179 at C2′ and C1′ (Figure 6); a possibility that finds support from analogous reactions in acetyl ADPR (Sauve et al., 2001). It is also notable that the electron density trails off near the phosphate group (Figure 7). Hydrolysis of the diphosphate bond of NAD would yield

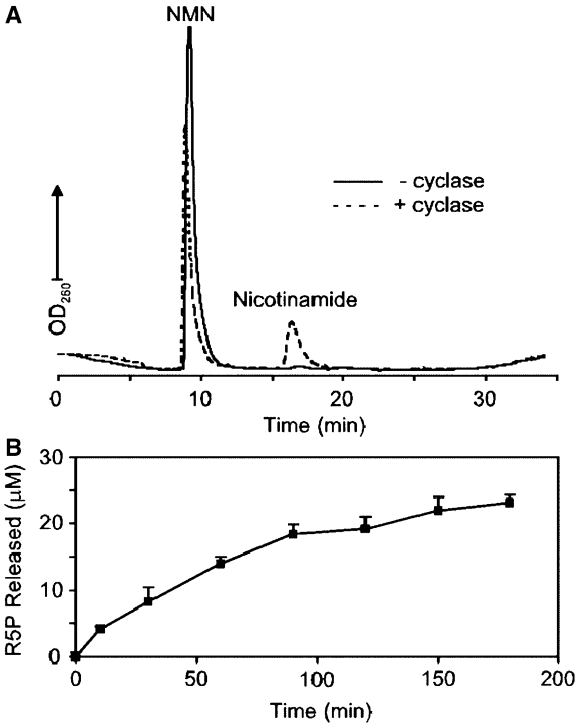

Figure 5. Hydrolysis of NMN to R5P Catalyzed by Cyclase

(A) NMN (0.1 mM) was incubated with the cyclase (1 μg/ml) at pH 5 (20 mM sodium acetate) for 3 hr at room temperature. Samples were analyzed by reversed phase HPLC on a C18 column.

(B) The time course of the release of R5P was measured by stopping aliquots of the reaction mixture with equal volume of charcoal (2% in 20 mM Tris-base and 2 mM $MgCl_2$). The activated charcoal bound up the NMN but not the product, R5P. After centrifuging for 5 min in a microfuge, the supernatants containing R5P released by the hydrolysis reaction were recovered and treated with alkaline phosphatase (10 U/ml) for 1 hr at 37°C. The amount of phosphate liberated from R5P was measured using the standard Malachite Green assay for inorganic phosphate.

the observed R5P, a reaction which is probably unrelated to cyclization, but which might be expected to occur in the time required for crystallization. It remains unclear whether the trailing density results from a residual amount of nonhydrolyzed diphosphate, NMN, or flexibility in the second phosphate with resulting disorder in the purine group of a bound NAD molecule. The C3′-Glu179 bond probably results from an intramolecular rearrangement that occurs between the ribose ring and the carboxylate moiety, when cyclization is blocked by pyridylcarbinol-class BES. When the substrate is present and unblocked, cyclization proceeds via the elimination of the carboxylate oxygen of Glu179 at C1′ of R5P, and the product is released. This is the end state observed in the crystals grown with NGD, where neither nicotinamide nor pyridylcabinol was added, and covalently bound R5P was not observed. (It should be noted that R5P binding was not observed in the Glu179Ala mutant structure either.) Overall, these results are consistent with the notion that cyclization proceeds through a covalently bound intermediate at Glu179. Moreover, these structures together show that the covalent intermediate can be captured using a BES, because BES

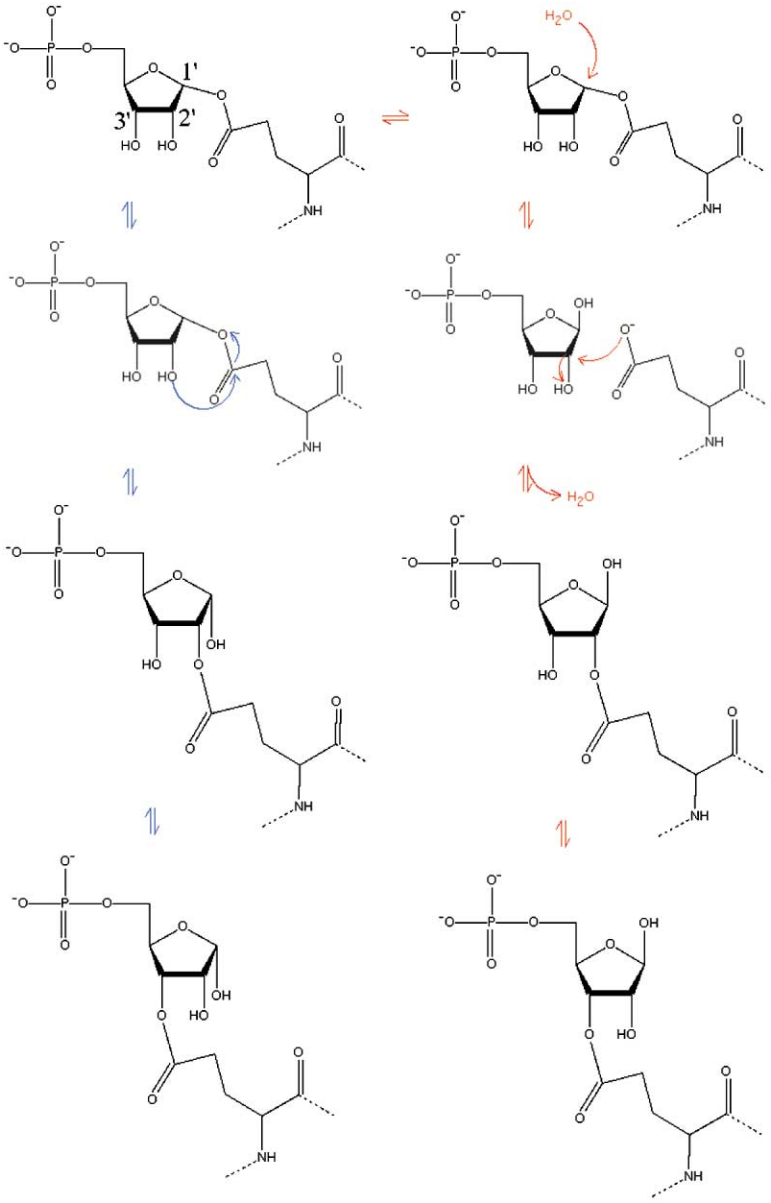

Figure 6. Two Proposed Mechanisms to Form 3′ Intermediate

The observed 3′ intermediate may be derived by at least two possible mechanisms, nonhydrolysis (blue) or hydrolysis (red). Hydrolysis is thought to occur at the 1′ position, but it is likely that certain analogous reactions can occur at the 2′ and 3′ positions as shown in the pathway to the right. It is also plausible that the intermediate pathway is an internal rearrangement that occurs without hydrolysis, shown at left, which is supported by similar 2′ and 3′ substitutions that occur in AADPR (Sauve et al. 2001). It should be noted that the 1′ hydroxyl is left in the up position via hydrolysis, but in the down position via internal rearrangement. From a mechanistic standpoint, this difference might clarify whether base exchange substrates block hydrolysis versus product release. Unfortunately, hydroxyl groups did not refine well in either configuration, and we are not able to distinguish these two possibilities at the current resolution of the data.

appears to block cyclization, and the covalent intermediate was not observed in the absence of BES. This conclusion is congruent with the similar effect of mechanism-based inhibitors on CD38 (Sauve and Schramm, 2002). Thus, it is now clear that covalent intermediate catalysis occurs in the course of the cyclization and base exchange reactions in the active site of *Aplysia* cyclase.

Comparison of high-resolution structures together with identification of the cyclase mechanism leads to a profound understanding of the residues that participate in the global reaction, and helps to explain the biochemical differences in the cyclase enzyme family. Homology-based models of CD38 constructed using the 3D-PSSM program (Kelley et al., 2000) assisted with this comparison (Figure 8). Cyclase residue Glu98 is conserved in CD38, but it appears as serine or cysteine in BST-1, and this variable residue also appears to be involved in the reaction (Graeff et al., 2001). In cyclase and in the CD38 model, the carboxylate group of Glu98 directly opposes C1′ and C2′ of the ribose ring with respect to Glu179 of the enzyme, and these moieties together form a geometric reaction plane (Figure 3). The Glu98 is a strong hydrogen bond acceptor because the charged group is mostly buried in the core of the enzyme beneath Trp77, and also geometrically stabilized by an internal salt bridge to His85. It is therefore likely that Glu98 provides stabilization for the hydrolysis reaction and for nicotinamide elimination at ribose C1′ by Glu179. Glu98 is also part of the nicotinamide binding site in the current structure and in BST-1 as well (Yamamoto-Katayama et al., 2002). The pyridylcarbinol-bound structure shows the interaction of Glu98 with the amine group of the aromatic ring in a manner similar to nicotinamide. After nicotinamide release, the purine group of the substrate must take its place in the binding site in order for cyclization

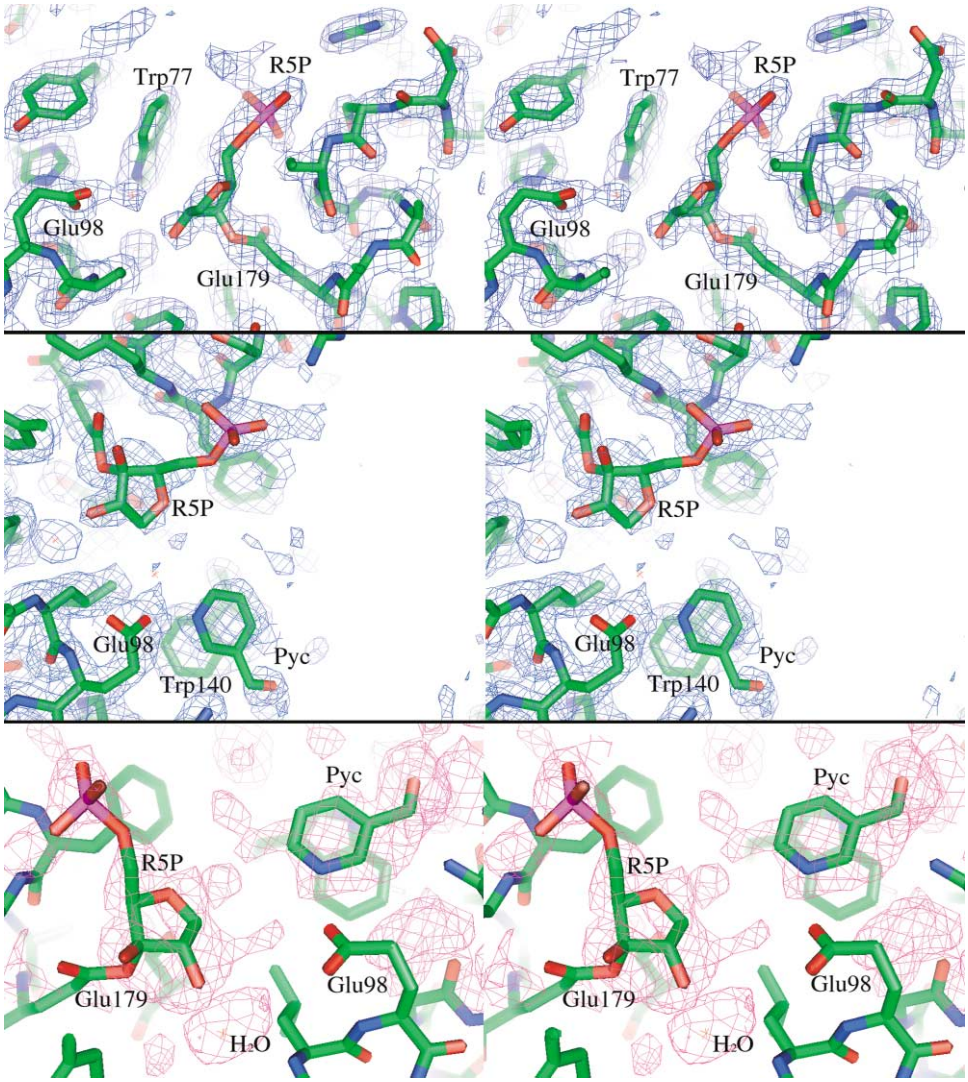

Figure 7. Electron Density Map

Ribose-5-phoshate (R5P) is covalently bound to Glu179, so that the residue spans a critical helix of the cyclase enzyme. In addition, the ribose ring makes contact with a nearby tryptophan residue (Trp77). In the top two panels, the final 2Fo-Fc electron density map, 1 σ, was calculated with the the program CNS (Brünger et al., 1998). In the middle panel, pyridylcarbinol (Pyc) is shown bound to Trp140 and Glu98. In the lower panel, a simulated annealing Fo-Fc omit map (pink) was calculated with R5P, Pyc, and an adjacent water molecule deleted from the structure. The omit map is shown at 1.7 σ. The figure was rendered with the program PyMOL (http://pymol.sourceforge.net).

to occur. Glu98 and Trp140 probably position the purine group of the substrate for nucleophilic attack on C1′ of the ribose ring, leading to elimination of the carboxylate oxygen of Glu179. Thus, Glu98 would promote cyclization of the substrate in a manner consistent with the formation of a covalent intermediate at Glu179 of the enzyme so long as the active site can be cleared of nicotinamide. (Similar arguments can be made in regard to residue Glu78 of BST-1, which would appear to block the phosphate interactions with the N terminus of the adjacent helix which are observed in cyclase and the CD38 model [Figure 8].) In this scheme, Glu 98 is a crucial residue for cyclization and nicotinamide binding specificity. The substitution of cysteine in place of glutamic acid at position 98, which appears in mouse BST-1, may lead to a loss of specificity for cyclization or nicotinamide binding with respect to other BST-1 and cyclase, and to hydrolysis of the substrate at C1′ of the ribose ring.

Another feature of the enzyme which might affect cyclization is the presence of a second nicotinamide binding site adjacent to the catalytic cleft. The second nicotinamide molecule is bound to Trp111 of the enzyme in the original cyclase structure (Figure 3), and the occupancy of this nicotinamide site appears to be higher than that of the initially observed site at Trp140 (which also corresponds to the pyridylcarbinol site). In BST-1 and in the CD38 model, this site is blocked by V136 and I133 respectively. It might be expected that a second nicotinamide site would assist cyclization and hydrolysis by shunting of nicotinamide out of the active site and clearing Trp140 for the binding of the purine group of

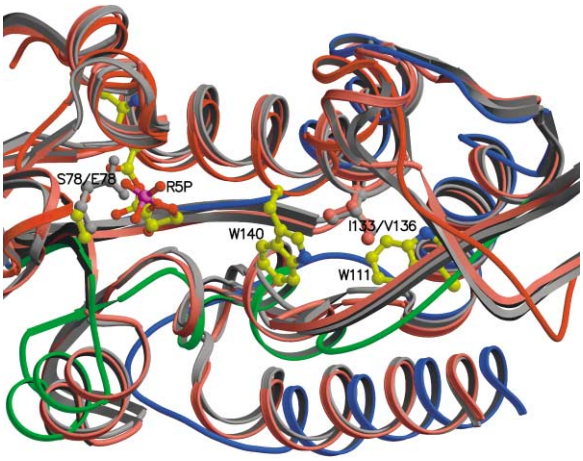

Figure 8. Comparison of Cyclase and BST-1 Structures and CD38 Model

The cyclase subunits are colored blue, green, and red, from the N- to C-terminal respectively, and the side chains are shown in ball-and-stick representation with yellow carbon, blue nitrogen, red oxygen, and violet phosphorus. BST-1 is colored gray, and the BST-1-based CD38 model is colored pink. E78 of BST-1 conflicts with the phosphate group of R5P in the current structure, which may indicate an impeded tendency toward cyclization with respect to cyclase and CD38, both of which have a serine residue in this position. The CD38 model is more similar to cyclase than to BST-1 in the region of the cyclization cleft surrounding R5P (cyclase-based model not shown). In contrast, CD38 and BST-1 are similar in the region of the second nicotinamide site of cyclase in that W111 is blocked by I133 or V136 respectively. Thus, it appears that CD38 shares properties affecting cyclization with cyclase, but CD38 also shares properties affecting nicotinamide binding with BST-1. The proteins are shown in ribbon representations. Key residues appear as ball-and-stick, and the N-terminal loops are truncated at the first helix for clarity purposes. The figure was rendered with the program Raster3D (Merritt and Bacon, 1997).

the cyclization substrate. Thus, an analysis of the current structures predicts that CD38 would be similar to BST-1 in nicotinamide binding, but nicotinamide release at Trp140 would be similar to cyclase due to the presence of the crucial residue, Glu98.

Structural Comparison of Enzymatic Mechanisms for Cyclase, CD38, and BST-1

These high-resolution structures, combined with comparison to the structure of BST-1 (Yamamoto-Katayama et al., 2002) and to our CD38 model, have provided for a detailed understanding of the cyclization mechanism and a structural explanation of the relative enzymatic differences which supports the known biochemical properties of this crucial protein family. In particular, the differentiation of relative tendency toward cyclization versus hydrolysis and stabilization of the covalent intermediate can all be explained based on the structures and on specific sequence differences. Overall, the CD38 model shares one of two cyclization-promoting properties with cyclase: it has a strong hydrogen bond accepor (Glu98) near the active site but not a second nicotinamide site, so that CD38 is expected to have similar cyclization and hydrolysis chemistry to cylase, but different nicotinamide binding properties. In this mechanistic scheme, mouse BST-1 does not share either property with cyclase, so that the cyclization reaction is impaired with respect to both CD38 and cyclase. The identification of a BES trapped covalent intermediate implies that BES release may play a role in determining cyclization versus hydrolysis; it is unclear how BES binding to Trp140 blocks hydrolysis, such binding apparently blocks cyclization sterically.

A general reaction model for the protein family proceeds from the understanding of the enzymatic mechanism of cyclase, and future experiments can be proposed which will better explain the biochemical differences between cyclase, CD38, and BST-1. For example, nicotinamide binding properties can be assayed with tryptophan fluorescence experiments. General cyclization and hydrolysis inhibitors might target the innermost nicotinamide site which is shared by all the proteins in this family. ADP-ribosyl cyclase activity can presumably be modulated by agents designed to specifically target the second nicotinamide site, which may reduce cyclic product while leaving other cyclase activities unaffected. Moreover, the pursuit of CD38 and additional inhibitor-bound structures at higher resolutions may lead to improved reagents and mechanistic insights, which could be of therapeutic interest.

Experimental Procedures

Crystallization, Data Collection, and Molecular Replacement

The preparation of triclinic nicotinamide-bound *Aplysia* ADP-ribosyl cyclase crystals with unit cell dimensions a = 60.4 Å, b = 75.3 Å, c = 138.1 Å, α = 88.2°, β = 89.2°, γ = 89.1°, and the details of data collection and molecular replacement solution were previously described (Munshi et al., 1999). Since that time, monoclinic cyclase crystals with unit cell dimensions a = 70.3 Å, b = 58.3 Å, c = 72.4 Å, β = 100.7° have been grown under conditions similar to the triclinic crystals and in the presence of the BES compounds, such as pyridylcarbinol, or in the presence of NGD. The monoclinic crystals were grown by seeding at 18°C from a mixture of 2 μl protein solution and 2 μl reservoir solution (0.1 M imidazole [pH 7.5] and 12%–24% PEG 4K). The partial specific volume (Matthews, 1968) was similar for both crystal forms (2.7 for triclinic, 2.5 for monoclinic), corresponding to eight and two molecules of 29 kDa per asymmetric unit respectively for the triclinic and monoclinic crystals. The monoclinic structures were solved by molecular replacement with the program AMoRe (Navaza, 1994), using the original cyclase structure (Prasad et al.l., 1996) as a search model, and the triclinic nicotinamide-bound structure (Munshi et al., 1999) has been refined to finality. All data were collected at MacCHESS with λ = 0.93 Å on beamline stations A1 and F1 using a Quantum 4 CCD detector, and the statistics of data collection and unit cell parameters are shown in Table 1.

Structural Refinement and Quality

The crystallographic refinement, molecular modeling and building, and molecular graphics calculations were performed using an Apple dual-processor G4 minicluster running the GNU-Darwin Distribution (http://www.gnu-darwin.org/). After an initial round of maximum likelihood positional refinement and simulated annealing using the program CNS (Brünger et al., 1998), the R factor fell to levels indicating a correct solution (25.21%, 25.74%, 25.72%, and 26.96% for the pyridylcarbinol-bound, nicotinamide-bound, native, and mutant structures respectively). The various ligands were built into the resulting simulated annealing omit maps, and a regimen of maximum likelihood phase refinement was applied, followed by an automated refinement procedure using ARP/WARP (Lamzin and Wilson, 1993) combined with multicrystal and noncrystallographic symmetry averaging using the program DM (Cowtan, 1994). The program PyMOL (http://pymol.sourceforge.net) was used for crystallographic struc-

Table 1. Data Collection and Refinement Statistics

Data Collection Statistics[a]

	Pyridylcarbinol	Nicotinamide[b]	Native	Mutant
Resolution range (Å)	24–2.0 (2.1–2.0)	33–2.4 (2.6–2.4)	25–1.7 (1.8–1.7)	20–2.0 (2.1–2.0)
R_{sym} (%)	9.0 (20.0)	10.8 (31.0)	5.4 (28.0)	8.6 (25.5)
Completeness (%)	99.5 (96.6)	88.0 (44.7)	99.1 (99.1)	99.7 (98.6)
Redundancy	3.4	3.9	3.3	3.8

Crystallographic Parameters

	a	b	c	α	β	γ	Space Group
Pyridylcarbinol	70.3 Å	58.3 Å	72.4Å	90°	100.7°	90°	P21
Nicotinamide[b]	60.4 Å	75.3 Å	138.1Å	88.2°	89.2°	89.1°	P1
Native	70.3 Å	58.3 Å	72.4Å	90°	100.8°	90°	P21
Mutant	70.3 Å	58.3 Å	72.4Å	90°	100.7°	90°	P21

Crystallographic Refinement Statistics

	Pyridylcarbinol	Nicotinamide[b]	Native	Mutant
Number of reflections	38,943	57,197	61,981	35,252
Sigma cutoff	none	none	none	none
R factor (%)	21.20	24.39	20.77	22.94
Free R factor (%)	25.18	26.94	23.79	26.13
Monomers per asymmetric unit	2	8	2	2
Ligands	R5P, pyridylcarbinol	R5P, nicotinamide	none	none
Total number of waters	92	0	276	66
Rms deviation from ideal				
Bond lengths (Å)	0.0179	0.0139	0.0185	0.0152
Bond angles (°)	1.8143	1.6915	1.8650	1.727

[a] Outer shell statistics in parentheses.
[b] Munshi et al. (1999).

ture building. In the last step, the models were refined using CNS and display good stereochemistry as judged by the programs CNS and PROCHECK (Laskowski et al., 1993). The final refinement and stereochemical statistics are shown in Table 1.

The automated refinement procedure in combination with averaging produced striking improvements in the electron density map, so that ribose-5-phosphate was clearly identified in the catalytic groove of the pyridylcarbinol- and nicotinamide-bound enzymes (Figure 7). A large number of protomers were available for averaging; eight per asymmetric unit in the nicotinamide-bound structure and two per asymmetric unit in the monoclinic crystals. It appears that the sugar interacts with the catalytic groove adjacent to the nicotinamide site (Munshi et al., 1999). This observation is supported by the observation of reagent hydrolysis in ADP-ribosyl cyclase (Figure 5), and by the recently published BST-1 structures (Yamamoto-Katayama et al., 2002). C3′ of the sugar forms a covalent linkage with Glu179, consistent with the observation that this residue participates in a covalent intermediate as part of the ADP-ribosylation and cyclization reaction in the homologous enzyme CD38 (Sauve and Schramm, 2002; Sauve et al., 2000). Moreover, residues Glu98 and His85 form an internal salt bridge near the active site, and may function as a hydrogen bond acceptor in the cyclization reaction.

The structure of cyclase crystals grown in the presence of NGD was determined to 1.7 Å resolution, which provides the most detailed view of the enzyme to date, although the active site showed no substrate density. Inactive cyclase mutant Glu179Ala was also determined to 2.0 Å resolution, and the structure was similar to that of the native protein, which would imply that Glu179 plays an enzymatic role, but not a structural role.

Acknowledgments

This work was supported by grants from the NIH to H.C.L. (GM6033) and MacCHESS (RR01646). The data were collected at the Cornell High Energy Synchrotron Source (CHESS), which is supported by the NSF and NIH National Institute of General Medical Sciences under award DMR 9713424.

Received: April 25, 2003
Revised: November 12, 2003
Accepted: November 13, 2003
Published: March 9, 2004

References

Aarhus, R., Graeff, R.M., Dickey, D.M., Walseth, T.F., and Lee, H.C. (1995). ADP-ribosyl cyclase and CD38 catalyze the synthesis of a calcium-mobilizing metabolite from NADP. J. Biol. Chem. *270*, 30327–30333.

Brünger, A.T., Adams, P.D., Clore, G.M., Delano, W.L., Gros, P., Grosse-Kuntsleve, R.W., Jiang, J.-S., Kuszewski, J., Nilges, N., Pannu, N.S., et al. (1998). Crystallography and NMR system (CNS): a new software system for macromolecular structure determination. Acta Crystallogr. D Biol. Crystallogr. *54*, 905–921.

Cowtan, K. (1994). "DM." An automated procedure for phase improvement by density modification. Joint CCP4 and ESF-EACBM Newsletter on Protein Crystallography *31*, 34–38.

Dong, C., Wang, J., Neame, P., and Cooper, M.D. (1994). The murine BP-3 gene encodes a relative of the CD38/NAD glycohydrolase family. Int. Immunol. *6*, 1353–1360.

Graeff, R., Munshi, C., Aarhus, R., Johns, M., and Lee, H.C. (2001). A single residue at the active site of CD38 determines its NAD cyclizing and hydrolyzing activities. J. Biol. Chem. *276*, 12169–12173.

Harada, N., Santos-Argumedo, L., Chang, R., Grimaldi, J.C., Lund, F.E., Brannan, C.I., Copeland, N.G., Jenkins, N.A., Heath, A.W., Parkhouse, R.M., et al. (1993). Expression cloning of a cDNA encoding a novel murine B cell activation marker. Homology to human CD38. J. Immunol. *151*, 3111–3118.

Itoh, M., Ishihara, K., Tomizawa, H., Tanaka, H., Kobune, Y., Ishikawa, J., Kaisho, T., and Hirano, T. (1994). Molecular cloning of murine BST-1 having homology with CD38 and *Aplysia* ADP-ribosyl cyclase. Biochem. Biophys. Res. Commun. *203*, 1309–1317.

Jackson, D.G., and Bell, J.I. (1990). Isolation of a cDNA encoding

the human CD38 (T10) molecule, a cell surface glycoprotein with an unusual discontinuous pattern of expression during lymphocyte differentiation. J. Immunol. *144*, 2811–2815.

Kaisho, T., Ishikawa, J., Oritani, K., Inazawa, J., Tomizawa, H., Muraoka, O., Ochi, T., and Hirano, T. (1994). BST-1, a surface molecule of bone marrow stromal cell lines that facilitates pre-B-cell growth. Proc. Natl. Acad. Sci. USA *91*, 5325–5329.

Kelley, L.A., MacCallum, R.M., Sternberg, M.J. (2000) Enhanced genome annotation using structural profiles in the program 3D-PSSM. J. Mol. Biol. *299*, 499–520.

Koguma, T., Takasawa, S., Tohgo, A., Karasawa, T., Furuya, Y., Yonekura, H., and Okamoto, H. (1994). Cloning and characterization of cDNA encoding rat ADP-ribosyl cyclase/cyclic ADP-ribose hydrolase (homologue to human CD38) from islets of Langerhans. Biochim. Biophys. Acta *1223*, 160–162.

Kraulis, P.J. (1991). MOLSCRIPT: a program to produce both detailed and schematic plots of protein structures. J. Appl. Crystallogr. *24*, 946–950.

Lamzin, V.S., and Wilson, K.S. (1993). Automated refinement of protein models. Acta Crystallogr. D Biol. Crystallogr. *49*, 129–147.

Laskowski, R.A., MacArthur, M.W., Moss, D.S., and Thornton, J.M. (1993). PROCHECK: a program to check the stereochemical quality of structures. J. Appl. Crystallogr. *26*, 283–291.

Lee, H.C. (1991). Specific binding of cyclic ADP-ribose to calcium-storing microsomes from sea urchin eggs. J. Biol. Chem. *266*, 2276–2281.

Lee, H.C. (1996). Cyclic ADP-ribose and calcium signaling in eggs. Biol. Signals *5*, 101–110.

Lee, H.C. (2001). Physiological functions of cyclic ADP-ribose and NAADP as calcium messengers. Annu. Rev. Pharmacol. Toxicol. *41*, 317–345.

Lee, H.C., Aarhus, R., and Walseth, T.F. (1993). Calcium mobilization by dual receptors during fertilization of sea urchin eggs. Science *261*, 352–355.

Lee, H.C., Aarhus, R., and Levitt, D. (1994). The crystal structure of cyclic ADP-ribose. Nat. Struct. Biol. *1*, 143–144.

Lee, H.C., Graeff, R., and Walseth, T.F. (1995). Cyclic ADP-ribose and its metabolic enzymes. Biochimie *77*, 345–355.

Li, Q., Yamada, Y., Yasuda, K., Ihara, Y., Okamoto, Y., Kaisaki, P.J., Watanabe, R., Ikeda, H., Tsuda, K., and Seino, Y. (1994). A cloned rat CD38-homologous protein and its expression in pancreatic islets. Biochem. Biophys. Res. Commun. *202*, 629–636.

Matthews, B.W. (1968). Solvent content of protein crystals. J. Mol. Biol. *33*, 491–497.

Merritt, E.A., and Bacon, D.J. (1997). Raster3D photorealistic molecular graphics. Methods Enzymol. *277*, 505–524.

Munshi, C., Thiel, D.J., Mathews, I.I., Aarhus, R., Walseth, T.F., and Lee, H.C. (1999). Characterization of the active site of ADP-ribosyl cyclase. J. Biol. Chem. *274*, 30770–30777.

Navaza, J. (1994). AMoRe: an automated package for molecular replacement. Acta Crystallogr. A *50*, 157–163.

Prasad, G.S., McRee, D.E., Stura, E.A., Levitt, D.G., Lee, H.C., and Stout, C.D. (1996). Crystal structure of *Aplysia* ADP-ribosyl cyclase, a homologue of the bifunctional ectozyme CD38. Nat. Struct. Biol. *3*, 957–964.

Sauve, A.A., and Schramm, V.L. (2002). Mechanism-based inhibitors of CD38: a mammalian cyclic ADP-ribose synthetase. Biochemistry *41*, 8455–8463.

Sauve, A.A., and Schramm, V.L. (2003). Sir2 regulation by nicotinamide results from switching between base exchange and deacetylation chemistry. Biochemistry *42*, 9249–9256.

Sauve, A.A., Deng, H., Antelleti, R.H., and Schramm, V.L. (2000). A covalent intermediate in CD38 is responsible for ADP-ribosylation and cyclization reactions. J. Am. Chem. Soc. *122*, 7855–7860.

Sauve, A.A., Celic, I., Avalos, J., Deng, H., Boeke, J.D., and Schramm, V.L. (2001). Chemistry of gene silencing: the mechanism of NAD+-dependent deacetylation reactions. Biochemistry *40*, 15456–15463.

States, D.J., Walseth, T.F., and Lee, H.C. (1992). Similarities in amino acid sequences of *Aplysia* ADP-ribosyl cyclase and human lymphocyte antigen CD38. Trends Biochem. Sci. *17*, 495.

Wallace, A.C., Laskowski, R.A., and Thornton, J.M. (1995). LIGPLOT: a program to generate schematic diagrams of protein-ligand interactions. Protein Eng. *8*, 127–134.

Willmott, N., Sethi, J.K., Walseth, T.F., Lee, H.C., White, A.M., and Galione, A. (1996). Nitric oxide-induced mobilization of intracellular calcium via the cyclic ADP-ribose signaling pathway. J. Biol. Chem. *27*, 3699–3705.

Yamamoto-Katayama, S., Ariyoshi, M., Ishihara, K., Hirano, T., Jingami, H., and Morikawa, K. (2002). Crystallographic studies on human BST-1/CD157 with ADP-ribosyl cyclase and NAD glycohydrolase activities. J. Mol. Biol. *316*, 711–723.

Accession Numbers

Protein structures have been deposited in the Protein Data Bank (accession codes: 1R16 [pyridylcarbinol], 1R15 [nicotinamide], 1R12 [native], and 1R0S [mutant]).